Ab initio Simulation of the Grafting of Phenylacetylene on Hydrogenated Surfaces of Crystalline Silicon Catalyzed by a Lewis Acid

Federico Zipoli and Marco Bernasconi*

Dipartimento di Scienza dei Materiali, Università di Milano-Bicocca, Via Cozzi 53, I-20125, Milano, Italy

Received: July 17, 2006; In Final Form: September 18, 2006

Car−Parrinello simulations have been carried out to identify the grafting mechanism of phenylacetylene, a prototypical alkyne, on the hydrogenated surfaces of crystalline silicon, catalyzed by a Lewis acid ($AlCl_3$). To this purpose, we have made use of a new technique, metadynamics, devised recently to deal with complex chemical reactions in first principles simulations. The reaction mechanism, leading to a styrenyl-terminated surface, turns out to be equivalent to the corresponding gas-phase hydrosilylation reaction by silanes that we have identified in a previous work. The activation energies for the surface reactions (0.43, 0.42, 0.35 eV, for H−Si(111), H−Si(100)2 × 1, and H−Si(100)1 × 1, respectively) are very close to that of the corresponding gas-phase reaction (0.37 eV). The estimated activation free energy at room temperature is sufficiently low for the grafting reaction to be viable at normal conditions and at low coverage on the crystalline silicon surfaces, as already well documented to occur on the surface of porous silicon. However, the conformation of the transition state shadows a large area of the surface, which might contribute to making the grafting process self-limiting.

I. Introduction

There is a rapidly growing interest in the study of the interaction of organic molecules with silicon surfaces in the perspective use of functionalized silicon surfaces for sensor and molecular electronic applications.[1,2] Different strategies have been proposed to graft organic molecules on crystalline silicon with the formation of a Si−C bond. Functionalization of the clean silicon surfaces in ultrahigh vacuum (UHV) conditions offers the possibility of controlling the surface morphology and the grafting mechanism at the atomic level and imaging the surface-bonded molecules by STM.[3] However, the use of UHV conditions for device fabrication is hampered by obvious difficulties to scale-up the whole process at the industrial level. Several other approaches offer alternative routes to surface functionalization, ranging from the use of thermal treatments,[4−8] UV[5,9−14] and visible light[15,16] irradiation, electrochemistry,[17,18] and wet chemical approaches such as reactions of carbanions from organolithium or Grignard reactants in ether solvent[19−21] or hydrosilylation reactions mediated by Lewis acids in nonpolar solvents (hydrocarbons).[22,21] Hydrosilylation reactions mediated by Lewis acids such as $AlCl_3$ or Et_2AlCl have been proposed on the basis of the corresponding reactions using silanes and alkynes in the gas phase or in hydrocarbon solutions where a trans addition has been observed with high yield at 0 °C and high regio- and stereoselectivity.[23,24] Grafting via hydrosilylation reactions has been demonstrated on the surface of porous silicon[25] at room temperature, but its viability on the crystalline silicon surfaces is unclear. Hydrosilylation reactions mediated by Lewis acids have been investigated only for alkenes on the hydrogenated Si(111) surface.[22,21] Functionalization was reported at first at high temperatures (100 °C for 18 h) by Boukherroub et al.[22] However, later work by Webb and Lewis[21] showed that the Si(111) surface oxidizes in air more rapidly when alkylation is assisted by Lewis acids than when Grignard reagents are used, suggesting that a lower coverage is obtained via hydrosilylation. Differences in the behavior of the single-crystal H−Si(111) surface and porous silicon have been ascribed either to the presence of particular silicon hydride sites or to a lower resistance to coupling between the surface and the catalyst on porous silicon.[21] The mechanism itself of the surface hydrosilylation is assumed to be equivalent to the corresponding gas-phase reaction, which although plausible, it is speculative.[21]

In this paper, we study from first principles the grafting reaction of organic molecules on crystalline silicon aiming at identifying the detailed mechanism of the grafting process, assisted by Lewis acids. Besides the H−Si(111) surface, we have also considered the Si(100) face mono- or dihydrogenated, which is the technologically relevant substrate suitable to be produced with very low roughness.[6] No experimental data are available on the grafting mediated by Lewis acids on the latter surface. By means of ab initio Car−Parrinello simulations, we also aim at investigating possible different reactivities of the different surfaces. Instead of alkenes, studied in the experimental work of ref 21 on the H−Si(111) surface, here we consider alkynes that are supposed to be more reactive.[25] As a prototypical alkyne, we have chosen phenylacetylene (PhC_2H), which is the simplest alkyne with a functional group (the aryl group) suitable to be used for molecular recognition in a gas sensing device made of an organic monolayer on silicon.[26] Although $EtAlCl_2$ and Et_2AlCl are often used as hydrosilylation catalysts because of their high solubility in hydrocarbons, here we have considered the simpler $AlCl_3$.[23,24] This choice has been motivated by a possible lower computational cost of $AlCl_3$ because the ethyl groups of $EtAlCl_2$ and Et_2AlCl with slow librational motions might require longer simulation runs to observe the occurrence of the grafting reaction. To identify the path of the grafting process, we have made use of a new simulation technique, metadynamics,[27,28] developed recently to deal with rare events within Car−Parrinello molecular dynamics.

The reaction mechanism that emerged from the simulations is the same as that of the corresponding gas-phase reaction that

* Corresponding author. E-mail: marco.bernasconi@mater.unimib.it.

10.1021/jp064518m CCC: $33.50
Published on Web 10/31/2006

we have studied previously. Starting from the transformation paths identified by metadynamics, we have refined the geometry and the energy of the transition states by using a standard quantum chemical tool (P-RFO). The calculated activation barriers are in the 0.35−0.43 eV range, very close to the calculated value for the corresponding gas-phase reaction (0.37 eV).[29]

II. Method

Ab initio Car−Parrinello[30] molecular dynamics simulations have been performed within the framework of density functional theory in the local spin density approximation supplemented by generalized gradient corrections,[31] as implemented in the code CPMD.[32,33] Ultrasoft pseudopotentials,[34] plane wave expansion of Kohn−Sham (KS) orbitals up to a kinetic energy cutoff of 25 Ry, a fictitious electronic mass of 800 au, and a time step of 0.168 fs have been used. We have used the deuterium mass for hydrogen. Constant temperature (300 K) on ions is enforced by a Nosè−Hoover thermostat.[33] We have considered the hydrogenated Si(111) surface and the Si(100) surface both mono- and dihydrogenated.[35] The surfaces are modeled in a slab geometry with 3D periodic boundary conditions at the experimental lattice parameter of silicon (5.43 Å), which is 0.6% shorter than the theoretical one within our framework at full convergence in Brillouin Zone integration. Only the supercell Γ point has been considered in Brillouin Zone integration. The periodically repeated slabs are separated by vacuum, 11 Å wide. The (111) slab has 4 silicon layers, each containing 16 atoms. The (100) slab has 5 layers with 12 silicon atoms each (4 × 3 surface unit cells of H−Si(100)1 × 1). The top surface is either dihydrogenated (H−Si(100)1 × 1) or monohydrogenated with Si−Si surface dimers (H−Si(100)2 × 1). The H−Si(100)1 × 1 surface has been optimized in the canted geometry.[35] The bottom surface of the Si(111) slab is fully hydrogenated; the Si−H bonds are relaxed and kept fixed with the surface silicon atoms fixed at their bulk positions. The bottom surface of the Si(100) slab has been optimized in the canted geometry, and the SiH_2 groups are then kept fixed during the simulations. We have also checked that the energetics of the grafting process does not change (within 1 meV) by changing the configuration of the bottom surface from the canted geometry to the dihydrogenated ideal termination of the bulk (SiH_2 groups are optimized with symmetric Si−H bonds and silicon at its bulk position, see Figure 5c). The surface unit cell is sufficiently large to make the interaction of the adsorbing molecule (one per cell) with its periodic images negligible. The minimum H−H distance between two nearest periodic images is always larger than 10.5 Å. A similar framework has been used to study the grafting of organic molecules driven by a surface radical (Si•) on the H−Si(111) surface[36] or assisted by a photon on the surface of a silicon quantum dot.[37]

The hydrosilylation reaction we address here turns out to be an activated process with an energy barrier much larger than the thermal energy. Therefore, the reaction would not occur spontaneously during the short span of an ab initio MD run. To overcome this limitation, we have used the metadynamics technique devised recently, which allows large barriers to be overcome in an affordable simulation time (few picoseconds).[27,28,38−40] The method is based on coarse-grained, non-Markovian dynamics in the manifold spanned by few reaction coordinates biased by a history-dependent potential that drives the system toward the lowest saddle point. The main assumption is that the reaction path could be described on the manifold of few collective coordinates $S_\alpha(\{\boldsymbol{R}_I\})$, functions of the ionic coordinates $\boldsymbol{R}_I$. Following the scheme of ref 28, an additional dynamical variable s_α is associated to each $S_\alpha(\{\boldsymbol{R}_I\})$. The extended system is described by the Lagrangian

$$L = L_o + \sum_\alpha \frac{1}{2} M_\alpha \dot{s}_\alpha^2 - \sum_\alpha \frac{1}{2} k_\alpha (S_\alpha(\{\boldsymbol{R}_I\}) - s_\alpha)^2 - V(t, \{s_\alpha\}) \tag{1}$$

where L_o is the Car−Parrinello Lagrangian, the second term is the fictitious kinetic energy of the s_α, and the third term is a harmonic potential that restrains the value of the collective coordinates, $S_\alpha(\{\boldsymbol{R}_I\})$, to the corresponding dynamical collective variables, s_α. $V(t,\{s_\alpha\})$ in eq 1 is the history-dependent potential that is constructed by the accumulation of Gaussians, centered at the positions of the $\{s_\alpha\}$ already visited along the trajectory. The potential discourages the system from remaining in the region already visited and pushes it over the lowest energy barrier toward a new equilibrium basin. This method has been applied already to study chemical reactions at surfaces, in the gas phase and in the bulk.[29,40−44] In the simulation of the hydrosilylation reaction, we have used three collective variables: the coordination number of the aluminum atom (s1), the hydrogen atom (s2), and the silicon atom (s3) of a selected surface Si−H group with the two carbon atoms of the acetylenic bond, C_α and C_β. Following ref 28, the coordination number between atoms a and b is defined as

$$n_a = \sum_b \frac{1 - \left(\frac{r_{ab}}{d}\right)^p}{1 - \left(\frac{r_{ab}}{d}\right)^q} \tag{2}$$

where r_{ab} is the distance between the two atoms. The coordination number n_a estimates the number of atoms b within the bond cutoff distance to atom a and decays smoothly for larger distances. The exponents p and q have been chosen as 4 and 8 for s_1 and s_2, and 1 and 8 for s_3. We have chosen different exponents for s_3 because we need a long tail in the coordination between the reactive silicon and the two carbon atoms of the acetylenic bond. The scaling factor, d, is 1.8, 2.1, and 4.2 Å for the coordination numbers s_1, s_2, and s_3, respectively. The collective variable s_1 favors the formation of a $PhC_2H-AlCl_3$ adduct, whereas s_2 favors the hydrogenation of the organic molecule by silane. The third collective variable had to be introduced to favor the formation of the Si−C bond. No bias is introduced to force a regioselective hydrogenation or complexation by the catalyst. A sketch of the atoms involved in the definition of the collective variables is reported in Figure 1. We have chosen $M = 4.90\ 10^5$ au and $k = 1.0$ au in eq 1 and isotropic Gaussian functions to build the history-dependent potential with parameters $\delta s = 0.15$ and $W = 0.13$ eV.[27] All of the simulations started with the PhC_2H molecule flat above the surface with the center of the triple bond on top of the surface hydrogen atom involved in the reaction at a distance of ∼3 Å. The $AlCl_3$ molecule, in turn, is flat above the PhC_2H molecule with the Al atom ∼3 Å on top of the center of the acetylenic bond.

Although metadynamics allows one to compute activation energies from a finite temperature simulation, long simulation times (with small Gaussian height W) are needed to obtain accurate estimates of activation free energies. Actually, our metadynamics simulations are aimed at just obtaining a good starting guess for the transformation path. Then, the geometry

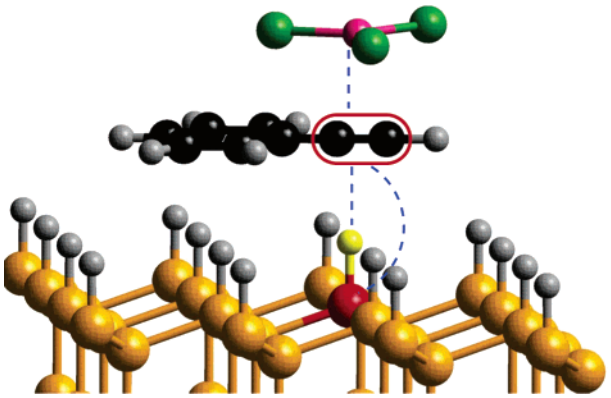

Figure 1. Sketch of the atoms involved in the definition of the collective variables for the reaction at the Si(111) surface. The blue dashed lines represent the three collective variables (see the text). The hydrogen and silicon atoms involved in the reaction are depicted with different colors with respect to the other surface atoms.

and activation energy of the transition state identified along the dynamical trajectory have been further refined by using a standard quantum standard chemical tool, the partitioned rational function optimizer (P-RFO).[45,46] We have verified that the geometry identified by the P-RFO method is indeed a saddle point by assigning a small kinetic energy (<10 meV) to the displacement pattern corresponding to the single negative eigenvalue of the Hessian matrix and by observing that the system evolves toward the products or reactants depending on the sign of the velocity pattern.

Entropic contributions ($T\Delta S$) to the activation free energy (ΔF) have been estimated for a selected case within the harmonic approximation from calculated phononic spectra of reactants and transition state (TS). Phonons in turn are obtained by diagonalization of the dynamical matrix at the Γ point, built from the numerical derivatives of the forces with respect to finite atomic displacements. From phonon calculations, we obtain the zero-point energy, ΔE_{zpe}, and the entropic contribution, ΔS, to the activation free energy as $\Delta S = k_B \ln(Z_{TS}/Z_{vib}Z_{rot})$ where, in turn Z_{TS} is the TS vibrational partition function (with the imaginary frequency omitted), Z_{vib} is the vibrational partition function of the isolated reactants ($PhC_2H-AlCl_3$ adduct and free surface), and Z_{rot} is the rotational partition function of the $PhC_2H-AlCl_3$ adduct. The translational contribution to the partition function of the gas-phase reactants that introduces a dependence of the rate on the reactant partial pressure is omitted.

We have not attempted to contrast the efficiency of the metadynamics technique with other well-established methods for the identification of the transition states, for example, the nudged-elastic-band (NEB) model.[47] However, for the application presented here, we might envisage two possible advantages of metadynamics. First, metadynamics allows one to identify the lowest transition state and thus the most probable product within a single simulation, as opposed to other techniques that would have required the calculation of the activation barrier for all of the possible regio- and steroisomers conceivable (however, with the byproduct additional information of the branching ratio). Second, metadynamics allows one to identify the transition state without a priori knowledge of the geometry of the final product. The latter information would instead be necessary for the application of the NEB method, and it would be particularly cumbersome to be obtained in the case of the catalyst-assisted reaction addressed here because the precise exit channel of the catalyst is unknown.

To visualize the electronic motion during the reaction, we use the centroids of the Wannier localized orbitals,[48,49] which

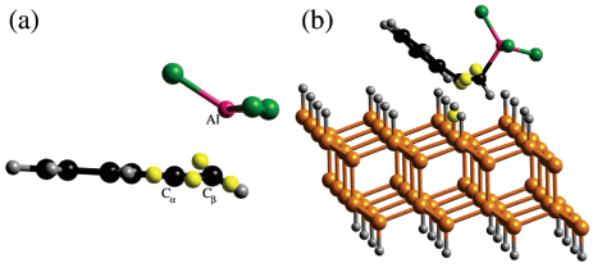

Figure 2. (a) Geometry of the bound $PhC_2H-AlCl_3$ adduct. The $C_\alpha-C_\beta$ bond length is 1.237 Å (1.215 Å in the isolated phenylacetylene). (b) Geometry of the transition state for the grafting of PhC_2H_2 on the H−Si(111) surface. The centroids of the Wannier orbitals involved in the hydrosilylation reaction are shown as small yellow spheres. Note that each sphere represents two electronic centroids for the α and β spins. A hydride is transferred from the surface Si−H group to the C_α carbon of the acetylenic bond.

are the periodic version of the Boys orbitals.[50] The Wannier orbitals are obtained by the unitary transformation of the Kohn−Sham occupied orbitals, which minimize the quadratic spread.[48,49]

III. Results

In a previous work,[29] we have used the framework outlined above to simulate the $AlCl_3$-mediated hydrosilylation of phenylacetylene by trimethylsilane ($HSiMe_3$) in the gas phase.

$$PhC{\equiv}CH + HSiMe_3 \xrightarrow{AlCl_3} PhCH{=}CHSiMe_3$$

A trans addition has been observed, leading to a *cis*-organosilane in agreement with experiments.[23,24] The simulation of the gas-phase reaction showed that the rate-determining step corresponds to the addition of H^- from the silane to the organic molecule in an anti-Markovnikov fashion. The calculated activation energy (0.37 eV)[29] is consistent with the high yield observed experimentally at 0 °C. The reaction mechanism identified theoretically coincides with that proposed speculatively in the experimental papers.[23,24] The simulation also revealed that the catalyst first coordinates the C_β atom of the acetylene bond, giving rise to a bound adduct 0.58 eV lower in energy that the sum of isolated PhC_2H and $AlCl_3$. The geometry of the adduct, identified in our previous work, is shown in Figure 2a. The aryl group bends upward slightly (CCC = 175.3°) in a "cis" configuration with the coordinated $AlCl_3$ molecule. Two electrons of the acetylenic bond move along the $C_\beta-Al$ bond (2.237 Å long) as shown by the centroid of the Wannier orbitals in Figure 2a. As a consequence, the C_α atom is electron-deficient and ready to accept the H^- anion from the silane. A similar adduct forms between PhC_2H and $EtAlCl_2$, but for a lower theoretical complexation energy (0.47 eV) and a longer $C_\beta-Al$ bond (2.32 Å long).

In the simulation of the hydrosilylation of phenylacetylene on the hydrogenated silicon surfaces addressed here, we have found a reaction path similar to that identified in the analogous gas-phase reaction. We have observed a hydrosilylation reaction of PhC_2H in a simulation run 3.3, 3.6, and 2.6 ps long for the H−Si(111), H−Si(100)2 × 1, and H−Si(100)1 × 1 surfaces, respectively. Pictures of the transition state and of the final product, a PhC_2H_2 grafted on the surface, are given in Figures 3−5, respectively for the H−Si(111), H−Si(100)2 × 1, and H−Si(100)1 × 1 surfaces. In the simulation, the $AlCl_3$ molecule goes away from the product because of the kinetic energy acquired during the formation of the Si−C bond. Analogous to the gas-phase reaction, the grafted molecule is a cis isomer that corresponds to a trans-hydrosilylation. The rate-determining step

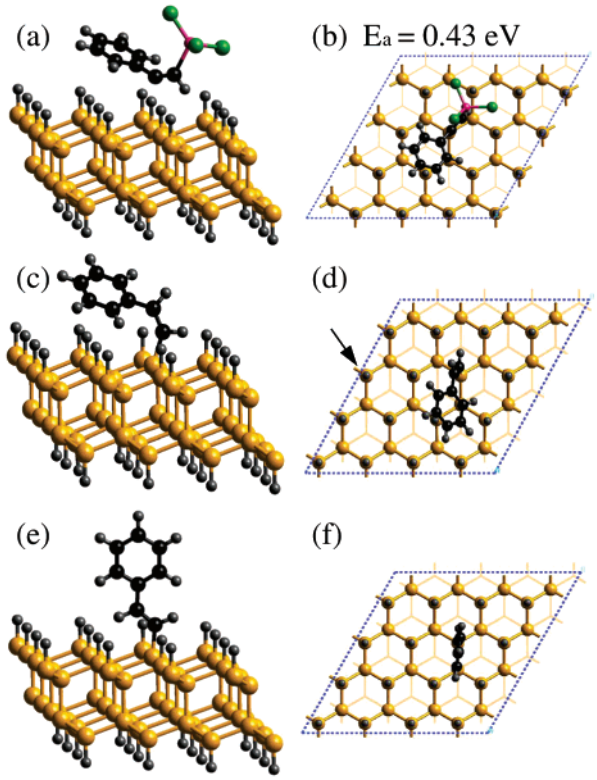

Figure 3. H−Si(111) surface: side (a) and top (b) views of the transition state. Side (c) and top (d) views of the final product, a PhC_2H_2 grafted on the surface in a cis geometry. Side (e) and top (f) views of PhC_2H_2 grafted on the surface in a trans geometry. The activation energy is given in panel b. The edges of the surface supercell are shown in the top views. The Si−C bond length and the SiĈC angle of the grafted molecule in the cis geometry are 1.880 Å and 138.7°. This configuration corresponds to a coverage of 1/16. The arrow in panel d shows the grafting site for a second molecule per cell introduced to model coverage 1/8 (see the text).

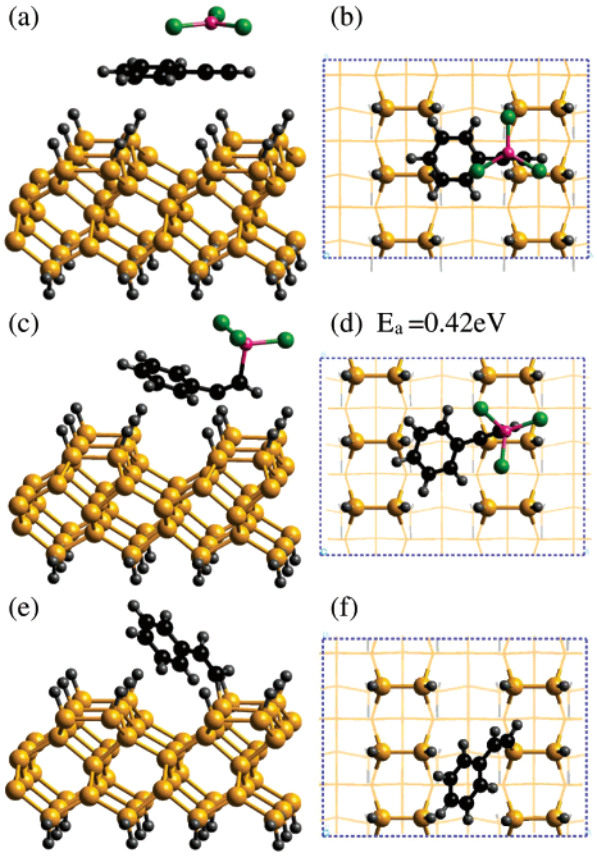

Figure 4. H−Si(100)2 × 1 surface: (a−b) reactants, (c−d) transition state, and (e−f) final product, a PhC_2H_2 grafted on the surface from a side and top views. The activation energy is given in panel d. The edges of the surface supercell are shown in the top views. The Si−C bond length and the SiĈC angle of the grafted molecule are 1.879 Å and 143.5°.

still consists of the transfer of the hydride (H^-) from the surface Si−H group to the electron-deficient C_α carbon of PhC_2H at the side opposite to $AlCl_3$ (Figures 3−5), that is, an anti-Markovnikov addition. The transfer of a hydride species is demonstrated by the analysis of the centroids of the Wannier orbitals shown in Figure 2b for the transition state on the H−Si(111) surface. The hydrocarbon solvent is not included in our simulation, but because the solvent is nonpolar we do not expect an important effect on the "ionic" transition state.

The geometry of the transition states shown in Figures 3−5 are obtained with the P-RFO method starting from the closest configuration in the dynamical trajectory. The main structural parameters of the transition states are given in Table 1 for the three surfaces. The potential energy felt by the transferred hydrogen atom around the saddle point is rather flat: the C_α−H distance can be increased by as much as 0.1 Å from the geometry of the saddle point with an energy gain of only 20 meV.

The activation energy with respect to the free surface and free $PhC_2H-AlCl_3$ adduct is 0.43, 0.42, and 0.35 eV for H−Si(111), H−Si(100)2 × 1, and H−Si(100)1 × 1 surfaces, respectively. A scheme of the energetics from reactants to products is reported in Figure 6. The physisorbed state of $PhC_2H-AlCl_3$ is not reported in Figure 6 because the physisorption energy is as small as 0.02 eV. The calculated activation energies for the surface reactions are all close to the activation energy (0.37 eV) for the hydrosilylation reaction of PhC_2H from a silane in the gas phase that we have obtained in our previous work.[29] For the H−Si(100)2 × 1 surface, we have estimated the zero point energy (ΔE_{zpe} = 0.096 eV) and the entropic contribution to the activation free energy as described in Section II. At 300 K (373 K), we obtain ΔF = 0.67 eV (0.70 eV). Given the similarities between the geometries and activation energies on the three surfaces, we might also expect similar activation free energies on the other surfaces. The calculated activation free energy appears to be sufficiently low to make the grafting of a single molecule (at low coverage) viable at normal conditions on the crystalline silicon surfaces. The difference in behavior between porous silicon and the H−Si(111) surface documented experimentally[21] should not come from a sizable difference in the reaction rate at low coverage but presumably from other effects self-limiting the grafting process as we will better argue below.

On the accuracy of the absolute values of the activation energies quoted above, we mention that benchmark calculations on the activation energy of a set of association reactions report a mean error on the order of 0.13 eV for PBE (and other GGA) functional.[51] The magnitude of the expected error is a large fraction of our absolute activation energies. However, we can argue that the viability at room temperature of the reactions investigated here is not supported only by the calculated absolute rate, which is affected by even larger errors due to large uncertainties in the rate prefactor, but can be better inferred from the similarity between the calculated activation energy of the surface reactions with that of the corresponding gas-phase reaction, which is known to occur with high yield at normal conditions.

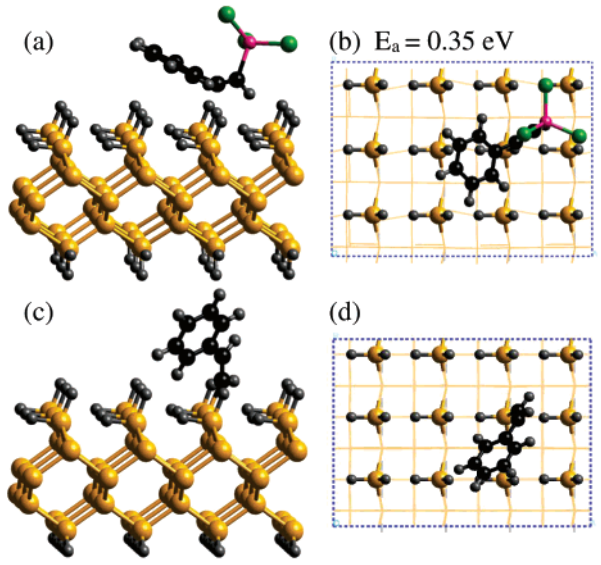

Figure 5. H−Si(100)1 × 1 surface: (a−b) transition state and (c−d) final product, a PhC_2H_2 grafted on the surface from a side and top views. The activation energy is given in panel b. The edges of the surface supercell are shown in the top views. The Si−C bond length and the SiĈC angle of the grafted molecules are 1.88 Å and 137°. Geometry optimizations have been repeated with the dihydrogenated bottom surface either in the canted geometry (panel a) or in the ideal termination of the bulk (panel c). The changes in the energetics of the grafting process are below 1 meV.

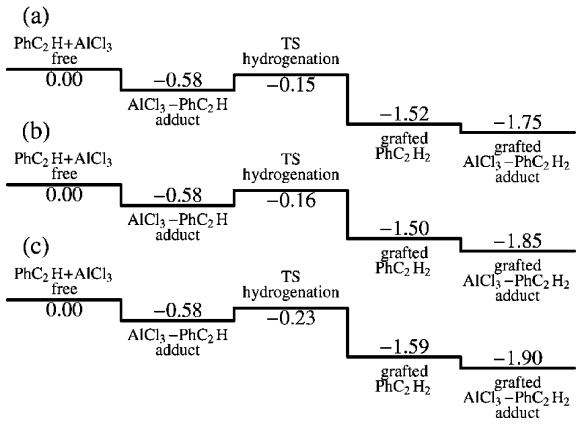

Figure 6. Energetics (eV) of the grafting process of phenylacetylene (PhC_2H) on the (a) H−Si(111), (b) H−Si(100)2 × 1, and (c) H−Si(100)1 × 1 surfaces. The transition state for the hydrogenation step (rate limiting) is indicated by TS. The last energy on the right corresponds to the grafted molecule with the catalyst bonded on the ethylenic double bond. The zero of energy corresponds to the unbound free PhC_2H and $AlCl_3$ molecules.

TABLE 1: Geometry of Transition States (cf. Figures 3−5)[a]

surface	C_α−H	Si−H	C_α−C_β	Si$\hat{C}_\alpha C_\beta$	Al−C_β	Si$\hat{H}C_\alpha$
H−Si(111)	1.474	1.626	1.289	104.0	2.079	169.2
H−Si(100)2 × 1	1.498	1.623	1.287	103.8	2.102	166.4
H−Si(100)1 × 1	1.539	1.597	1.284	111.8	2.095	156.3

[a] Bond lengths and bond angles are given in angstroms and degrees, respectively.

In the simulation and presumably in real life as well, the $AlCl_3$ molecule moves away from the product because of the kinetic energy acquired when the Si−C bond forms. However, analogous to the gas-phase reaction of alkynes and silanes,[29] a stable adduct between the Lewis acid and the grafted molecule can also form, albeit with a complexation energy (in the range 0.23−0.35 eV depending on the surface, cf. Figure 6) lower than the complexation energy with the free phenylacetylene (0.58 eV). The total energy of the grafted molecule with and without the bound catalyst are given in Figure 6. We note that the grafting energy is larger for the H−Si(100)2 × 1 surface and smaller for the H−Si(100)1 × 1 with an intermediate value for the H−Si(111) face. These differences in the grafting energy might originate from either the different strength of the Si−C bond on the different surfaces or the different steric coupling between the surface and the organic molecule. To further investigate this issue, we have optimized the geometry of phenylacetylene grafted in the trans conformation, which minimizes the steric coupling with the surface. We have also considered the simple acetylene molecule whose difference in grafting energies on the different surfaces would presumably come from slightly different Si−C bond strengths only. A picture of PhC_2H grafted in the trans geometry on H−Si(111) is given in Figure 3e−f. The corresponding pictures for the other surfaces and for acetylene are available as Supporting Information. The results on the grafting energies are summarized in Table 2; positive energies indicate exothermic grafting reactions. We note that the hierarchy in the grafting energies among the different surfaces is the same for simple acetylene and phenylacetylene in the trans geometry. Because for these molecules the steric coupling with the surface is small, we can ascribe the latter difference in the grafting energies to the different environment of the Si−C bond. The hierarchy in energy changes for phenylacetylene grafted in the cis geometry, which suggests that in this latter case most of the differences in the grafting energies come from a different steric coupling with the surface. In particular, the grafting energy is lower for H−Si(100)2 × 1 where the steric hindrance between the aryl group and the surface hydrogens is large.[52] On the H−Si(111) surface, we have also investigated the dependence of the grafting energy on the coverage. The configuration in Figure 3c and d corresponds to coverage 1/16. By doubling the coverage (1/8, see the caption of Figure 3d) the grafting energy does not change (within the figures given in Table 2) while at coverage 1/4 (Figure 7a) the grafting energy decreases slightly down to 1.50 eV/molecule. The geometry of the grafted molecules is very similar at all of the coverages considered. Steric repulsion between the grafted molecules is therefore negligible up to coverage 1/4.

TABLE 2: Grafting Energy (eV) of PhC_2H Bound in cis and trans Configurations and of Acetylene on the Three Surfaces[a]

	grafting energy (eV)		
surface	PhC_2H *cis*	PhC_2H *trans*	C_2H_2
H−Si(111)	1.52	1.90	1.97
H−Si(100)2 × 1	1.50	1.92	2.00
H−Si(100)1 × 1	1.59	1.85	1.95

[a] Positive energies indicate exothermic grafting reactions.

Coming back to the difference in behavior between porous silicon and the H−Si(111) surface documented experimentally in ref 21, on the basis of our calculations we would not expect a dramatically lower reaction rate on the crystalline surface with respect to porous silicon. However, experimentally it turns out that, as opposed to porous silicon, the coverage with organic molecules on H−Si(111) is lower when the grafting is mediated by a Lewis acid than when Grignard reactants on previous halogenated surface are used,[21] although the absolute reaction rates have not been measured for hydrosilylation reactions on crystalline silicon. As opposed to what was proposed in ref 21, the catalyst does not seem to experience a large steric resistance with the crystalline surface at low coverage. Actually, the catalyst is always rather far from the surface at the transition

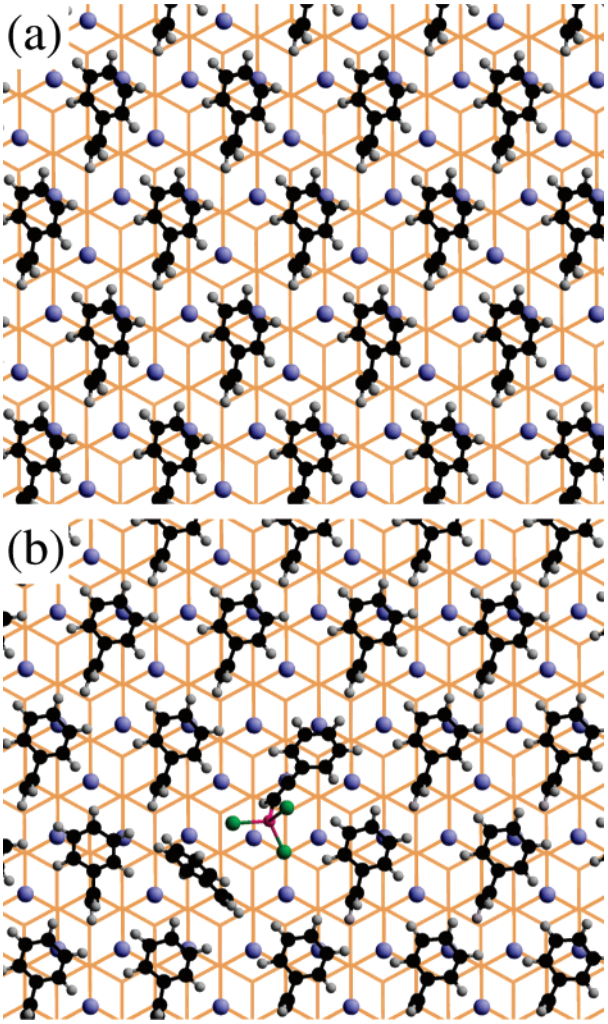

Figure 7. (a) Top view of the H−Si(111) surface with grafted PhC_2H_2 molecules at coverage 1/4, i.e., 25% of SiH groups substituted by the organic molecules. (b) The same as that in panel (a) with a single molecule substituted by the $PhC_2H-AlCl_3$ adduct in the transition-state geometry. This configuration is obtained by relaxing the system in a large supercell (30 grafted molecules) with classical force fields and fixing the geometry of the adduct in the transition state and of the substrate (see the text). As opposed to previous figures, only the hydrogen atoms of the surface Si−H groups (and not silicon atoms) are shown, depicted by (blue) spheres.

states in Figures 3−5. We can envisage that the higher coverage obtained by using the Grignard reagents might depend on the change in the surface morphology upon halogenation.[53] However, turning now on a more speculative level, we can also envisage that a larger steric hindrance might occur at higher coverage between the incoming alkyne−catalyst adduct and the already grafted molecules. The reason is twofold. First, for alkynes, the Lewis acid promotes the grafting only in the cis conformation (see Figures 3−5), which shadows more Si−H surface sites than the trans geometry (Figure 3e−f), which can be obtained by the Grignard-halogenation route. Second, the conformation of the transition state shadows even more Si−H sites. In Figure 7a we report a picture of the H−Si(111) surface with grafted phenylacetylene (cis) at a coverage of 1/4, at which no close contacts are present between the grafted molecules. However, at this coverage, by substituting a grafted molecule with the approaching adduct in the transition-state geometry we can easily recognize that the molecules already grafted have to rotate to reduce the steric hindrance with the incoming adduct. To model this effect, we have relaxed the large supercell (30 grafted molecules) shown in Figure 7b with the adduct of the last incoming molecule fixed in the transition-state geometry obtained from the simulation at low coverage. Because of computational limitations, the geometry optimization of this large system has not been obtained from first principles but by using two types of classical force fields[54,55] (with the software Cerius2 by Molecular Simulations Inc.) with very similar results. As shown in Figure 7b, only two molecules nearest neighbor to the adduct undergo sizable rotations. To reach the configuration of Figure 7a, these latter molecules have to overcome a rotational barrier that has been estimated from first principle at low (1/16) coverage in the supercell of Figure 3c and d. It turns out that the rotational barrier is 0.1 eV. An increase of the activation barrier of this order of magnitude would change the grafting rate by 2 orders of magnitude at room temperature. This effect might contribute to making the grafting process self-limiting at high coverage, and it would be even larger for the larger $EtAlCl_2$ and Et_2AlCl catalysts. A similar self-limiting effect might also be envisaged for the alkenes studied in ref 21. In fact, by assuming a similar grafting mechanism for alkyne and alkene hydrosilylation, the transition state for the reaction of alkenes would feature the plane defined by the reactive $H_2C{=}C$ group lying parallel to the surface. The "flat" ethylenic group with the catalyst bound to the CH_2 side would shadow several Si−H and thus experiences large steric hindrance with the already grafted molecules at high coverage forcing rotations of the already grafted molecules, as phenylacetylene does in Figure 7b. This self-limiting effect is probably less severe when the grafting is promoted by the carbanion of Grignard reactants, which can approach the halogenated surface "vertically".

IV. Summary and Conclusions

On the basis of ab initio Car−Parrinello simulations, we have identified the mechanism of the grafting of phenylacetylene, as a prototypical alkyne, on the crystalline, hydrogenated surfaces of silicon catalyzed by a Lewis acid ($AlCl_3$). The reaction mechanism turns out to be the same as that identified for the corresponding gas-phase reaction with silanes,[29] the rate-limiting step consisting of the transfer of the hydride (H^-) from the surface Si−H group to the C_α carbon of PhC_2H. The activation energies for the surface reactions (0.35−0.43 eV) are very close to that of the corresponding gas-phase reaction (0.37 eV). The three surfaces H−Si(111), H−Si(100)2 × 1, and H−Si(100)1 × 1 behave very similarly. The calculated activation energies are sufficiently low to predict high yield for the grafting at low coverage on the crystalline silicon surfaces as already well documented to occur on the surface of porous silicon. However, the conformation of the transition state shadows a large area of the crystalline surface, which might contribute to making the grafting process self-limiting on a flat crystalline surface.

Acknowledgment. We gratefully thank A. Laio, D. Narducci, and E. Romano for discussions and information. This work is partially supported by the INFM Parallel Computing Initiative, by CILEA, and by MURST through project PRIN03.

Supporting Information Available: A movie of the simulation on the H−Si(111) surface and pictures of grafted acetylene and phenylacetylene in the trans geometry. The movie refers to an additional simulation we have performed with different collective variables with respect to those discussed in the text, namely, the coordination number of Al with C_β and of Si with both C_α and C_β (two collective variables). This second choice does not change the transformation path, but allows one to

complete the reaction on a shorter simulation time and thus makes the movie file smaller. This material is available free of charge via the Internet at http://pubs.acs.org.

References and Notes

(1) Buriak, J. M. *Chem. Rev.* **2002**, *102*, 1271−1308.

(2) Wayner, D. D. M.; Wolkow, R. A. *J. Chem. Soc., Perkin Trans.* **2002**, *2*, 23−24.

(3) (a) Lopinsky, G. P.; Wayner, D. D. M.; Wolkow, R. A. *Nature (London)* **2000**, *406*, 48−51. (b) Lopinsky, G. P.; Wayner, D. D. M.; Wolkow, R. A. *Nature (London)* **1998**, *392*, 909−911.

(4) Sung, M. M.; Kluth, G. J.; Yauw, O. W., Maboudian, R. *Langmuir* **1997**, *13*, 6164−6168.

(5) Sieval, A. B.; Demirel, A. L.; Nissink, J. W. M.; Linford, M. R.; van der Maas, J. H.; de Jeu, W. H.; Zuilhof, H.; Sudholter, E. J. R. *Langmuir* **1998**, *14*, 1759−1768.

(6) Cerofolini, G. F.; Galati, C.; Reina, S.; Renna, L. *Semicond. Sci. Technol.* **2003**, *18*, 423−429.

(7) Sieval, A. B.; Opitz, R.; Maas, H. P. A.; Shoeman, M. G.; Meijer, G.; Vergeldt, F. J.; Zuilhof, H.; Sudholter, E. J. R. *Langmuir* **2000**, *16*, 10359−10368.

(8) Lehner, A.; Steinhoff, G.; Brandt, M. S.; Eickoff, M.; Stutzmann, M. *J. Appl. Phys.* **2003**, *94*, 2289−2294.

(9) Terry, J.; Linford, M. R.; Wigren, C.; Cao, R. Y.; Pianetta, P.; Chidsey, C. E. D. *Appl. Phys. Lett.* **1997**, *71*, 1056−1058.

(10) Terry, J.; Linford, M. R.; Wigren, C.; Cao, R. Y.; Pianetta, P.; Chidsey, C. E. D. *J. Appl. Phys.* **1999**, *85*, 213−221.

(11) Cicero, R. L.; Linford, M. R.; Chidsey, C. E. D. *Langmuir* **2000**, *16*, 5688−5695.

(12) Effenberger, F.; Gotz, G.; Bidlingmaier, B.; Wezstein, M. *Angew. Chem., Int. Ed.* **1998**, *37*, 2462−2464.

(13) Niederhauser, T. L.; Jiang, G. L.; Lua, Y. Y.; Dorff, M. J.; Woolley, A. T.; Asplund, M. C.; Berges, D. A.; Linford, M. R. *Langmuir* **2001**, *17* 5889−5900.

(14) Strother, T.; Cai, W.; Zhao, X. S.; Hamers, R. J.; Smith, L. M. *J. Am. Chem. Soc.* **2000**, *122*, 1205−1209.

(15) Sun, Q. Y.; de Smet, L. C. P. M.; van Lagen, B.; Wright, A.; Zuilhof, H.; Sudholter, E. J. R. *Angew. Chem., Int. Ed.* **2004**, *43*, 1352−1355.

(16) Yam, C. M.; Lopez-Romero, J. M.; Gu, J.; Cai, C. *Chem. Commun.* **2004**, *21*, 2510−2511.

(17) Fidelis, A.; Ozanam, F.; Chazalviel, J. N. *Surf. Sci.* **2000**, *444*, L7−L10.

(18) Allongue, P.; Delamar, M.; Desbat, B.; Fagebaume, O.; Hitmi, R.; Pinson, J.; Saveant, J.-M. *J. Am. Chem. Soc.* **1997**, *119*, 201.

(19) Kim, N. Y.; Laibinis, P. E. *J. Am. Chem. Soc.* **1999**, *121*, 7162−7163.

(20) Bansal, A.; Li, X. L.; Lauermann, I.; Lewis, N. S.; Yi, S. I.; Weinberg, W. H. *J. Am. Chem. Soc.* **1996**, *118*, 7225−7226.

(21) Webb, L. J.; Lewis, N. S. *J. Phys. Chem. B* **2003**, *107*, 5404−5412.

(22) Boukherroub, R.; Morin, S.; Bensebaa, F.; Wayner, D. D. M. *Langmuir* **1999**, *15*, 3831−3835.

(23) Sudo, T.; Asao, N.; Gevorgyan, V.; Yamamoto, Y. *J. Org. Chem.* **1999**, *64*, 2494−2499.

(24) Asao, N.; Sudo, T.; Yamamoto, Y. *J. Org. Chem.* **1996**, *61*, 7654−7655.

(25) Buriak, J. M.; Stewart, M. P.; Geders, T. W.; Allen, M. J.; Choi, H. C.; Smith, J.; Raftery, D.; Canham, L. T. *J. Am. Chem. Soc.* **1999**, *121*, 11491−11502.

(26) Narducci, D.; Bernardinello, P.; Oldani, M. *Appl. Surf. Sci.* **2003**, *212*, 491−496.

(27) Laio, A.; Parrinello, M. *Proc. Natl. Acad. Sci. U.S.A.* **2002**, *99*, 12562−12566.

(28) Iannuzzi, M.; Laio, A.; Parrinello, M. *Phys. Rev. Lett.* **2003**, *90*, 238302−238304.

(29) Zipoli, F.; Bernasconi, M.; Laio, A. *ChemPhysChem* **2005**, *6*, 1772−1775.

(30) Car, R.; Parrinello, M. *Phys. Rev. Lett.* **1985**, *55*, 2471−2474.

(31) Perdew, J. P.; Burke, K.; Ernzerhof, M. *Phys. Rev. Lett.* **1996**, *77*, 3865−3868.

(32) *CPMD V3.9*, Copyright IBM Corp (1990−2005) and MPI fuer Festkoerperforschung Stuttgart (1995−2001).

(33) Marx, D.; Hutter, J. In *Modern Methods and Algorithms of Quantum Chemistry*; Forschungszentrum Juelich, NIC Series, 2000; Vol. 1, p 301.

(34) Vanderbilt, D. *Phys. Rev. B* **1990**, *41*, 7892−7895.

(35) Tagami, K.; Tsuchida, E.; Tsukada, M. *Surf. Sci.* **2000**, *446*, L108−L112.

(36) Takeuchi, N.; Kanai, Y.; Selloni, A. *J. Am. Chem. Soc.* **2004**, *126*, 15890−15896.

(37) Reboredo, F. A.; Schwegler, E.; Galli, G. *J. Am. Chem. Soc.* **2003**, *125*, 15243−15249.

(38) Raiteri, P.; Gervasio, F. L.; Laio, A.; Micheletti, C.; Parrinello, M. *J. Phys. Chem. B* **2006**, *110*, 3533−3539.

(39) Laio, A.; Rodriguez-Fortea, A.; Gervasio, F. L.; Ceccarelli, M.; Parrinello, M. *J. Phys. Chem. B* **2005**, *109*, 6714−6721.

(40) Ensig, B.; Laio, A.; Parrinello, M.; Klein, M. L. *J. Phys. Chem. B* **2005**, *109*, 6676−6687.

(41) Churakov, S. V.; Iannuzzi, M.; Parrinello, M. *J. Phys. Chem. B* **2004**, *108*, 11567−11574.

(42) Stirling, A.; Iannuzzi, M.; Parrinello, M.; Molnar, F.; Bernhart, V.; Luinstra, G. A. *Organometallics* **2005**, *24*, 2533−2537.

(43) Stirling, A.; Iannuzzi, M.; Laio, A.; Parrinello M. *ChemPhysChem* **2004**, *5*, 1558−1568.

(44) Donadio, D.; Bernasconi, M. *Phys. Rev. B* **2005**, *71*, 73307.

(45) Billeter, S. R.; Curioni, A.; Andreoni, W. *Comput. Mater. Sci.* **2003**, *27*, 437−445.

(46) Banerjee, A.; Adams, N.; Simons, J.; Shepard, R. *J. Phys. Chem. B* **1985**, *89*, 52.

(47) Henkelman, G.; Jonsson, H. *J. Chem. Phys.* **2000**, *113*, 9978−9985.

(48) Marzari, N.; Vanderbilt, D. *Phys. Rev. B* **1997**, *56*, 12847−12864.

(49) Silvestrelli, P. L.; Marzari, N.; Vanderbilt, D.; Parrinello, M. *Solid State Commun.* **1998**, *107*, 7−11.

(50) Boys, S. F. *Rev. Mod. Phys.* **1960**, *32*, 296−299.

(51) Zhao, Y.; González-García, N.; Truhlar, D. G. *J. Phys. Chem. A* **2005**, *109*, 2012−2018.

(52) We have also performed a second simulation on the H−Si(100)2 × 1 surface from a starting configuration in which the reactants were rotated by 180° along the surface normal with respect to the configuration of Figure 4a. However, the $PhC_2H-AlCl_3$ adduct spontaneously rotates during the simulation to reach the transition state of Figure 4c.

(53) Pedemenonte, L.; Bracco, G.; Relini, A.; Rolandi, R.; Narducci, D. *Appl. Surf. Sci.* **2003**, *212*, 595−600.

(54) Mayo, S. L.; Olafson, B. D.; Goddard, W. A., III *J. Phys. Chem.* **1990**, *94*, 8897−8909.

(55) Rappe, A. K.; Casewit, C. J.; Colwell, K. S.; Goddard, W. A., III; Skiff, W. M. *J. Am. Chem. Soc.* **1992**, *114*, 10024−10035.